

Tutorial 3: *MD in NVE and NVT ensembles*

Michael Kopp (2439093)

1 Barrier Crossing

1.1 Continuous differentiable potential

In Order to have a potential $U = U(x)$ with differentiable U , U' and U'' , use

$$U(x) = \begin{cases} \varepsilon 2\pi^2 x^2 & x \leq 0 \\ \varepsilon(1 - \cos(2\pi x)) & 0 \leq x \leq 1 \\ \varepsilon 2\pi^2 (x - 1)^2 & x \geq 1 \end{cases}. \quad (1)$$

To see, how this potential looks like, cf. fig. 1. ε is some arbitrary energy parameter, in which the energies of the whole system will be measured, and x defines the unit to measure length in our system. You can think of x as in units of some physical system – e.g. some light field.

1.2 Reduced Units

These variables are kept abstract to preserve the scalability of the system. Some experimentalist conducting experiments can simply transfer his units into this ones by multiplying every length by the very length he measured in his system between the potential wells and multiplying every energy by the ε he measured in his system. You can imagine x as a ratio of r/σ where r is a measured distance and σ the characteristic length in the potential-landscape.

Later on we will measure temperatures, which will be done in units of mv^2 – thus in units of Energy –. The conversion factor in a real experiment should be something like the Boltzman-Factor k_B and the unit of temperatures thus is ε/k_B . Time is measured in $\sigma\sqrt{m/\varepsilon}$.

1.3 Particles in Potential (1) with different Temperatures

Since the Temperature is proportional to the cinetic energy of our single particle ($T \propto E_k$), the study of different temperatures is in fact a study of different kinetic energies at system-setup.

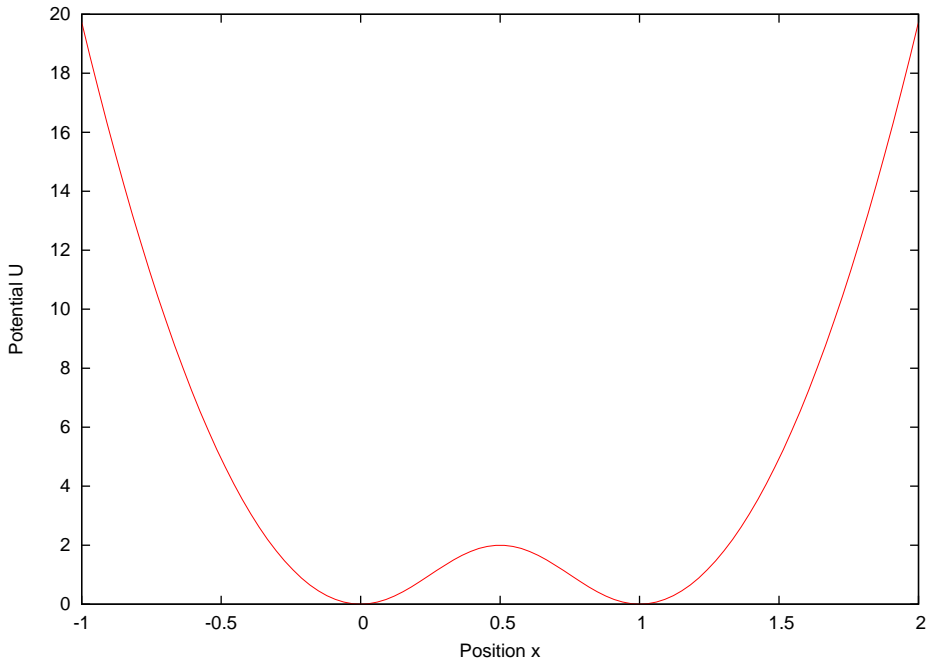


Figure 1: Potential from eq. (1)

For small kinetic energies, we must only consider a small displacement of the particle from the position of rest – thus we can use a Taylor-expansion of (1) to study the behaviour of the particle. With position of rest at $x = 0$ this yields

$$\varepsilon \left(2\pi^2 x^2 - \frac{2\pi^4 x^4}{3} + \mathcal{O}(x^6) \right)$$

for the $x \in [0, 1]$ -part and thus if we neglect potential-terms of order $\mathcal{O}(x^4)$ and higher we get the harmonic potential

$$U(x) \approx \varepsilon 2\pi^2 x^2 \quad \text{for } x \text{ near 0 .} \quad (2)$$

In fig. 2 one can see the x - E_k -diagram for a small temperature – namely $T = 0.05$ – to verify, that the system behaves like an harmonic oscillator (it's a sine). Next to that is a phase diagram of the system. The system forms a circle in a x - v -diagram. This is due to the fact that for an harmonic oscillator $v \propto \sin(\omega t)$ and $x \propto \cos(\omega t)$, so basically the diagram is the same as the unit circle, used to define sine and cosine.

In fig. 3 you can observe the different phase-diagrams for different temperatures. We can see here, that the approximation of eq. (2) is valid for

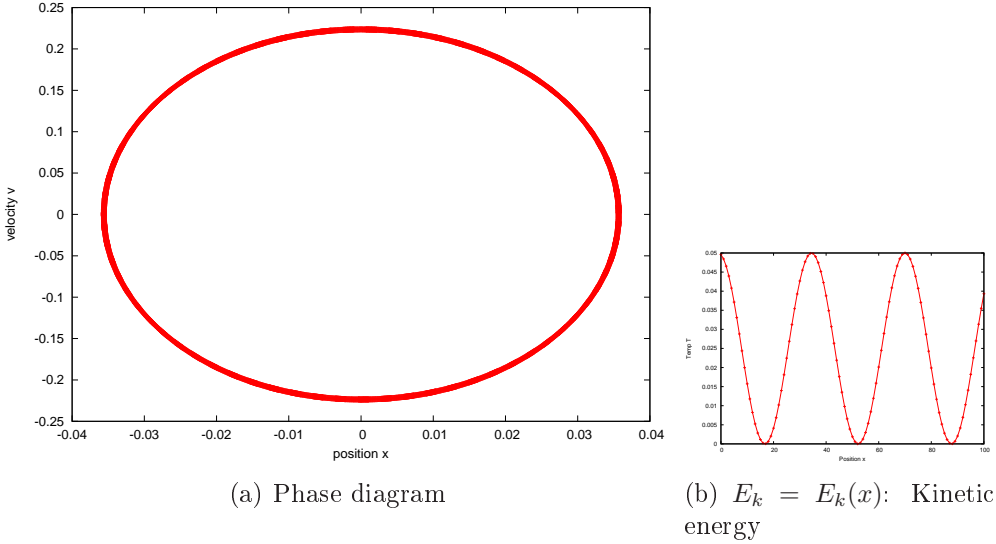


Figure 2: The System at $T = 0.05$

quite large temperatures – still for $T = 1.5$. To understand this, in fig. 4 both the potential (1) and it's Taylor-approx. (2) are plotted. Additionally the energies of the particles at the Temperatures used for fig. 3 are shown there, too. One can see, that 2 holds for $T = 1.5$ quite well.

For $T = 4.0$ one should expect, that the particle stops at the “hill” at $x = 0.5$. Looking at the output of the program more closely, the particle does so¹ – it remains quite long at $x = 0.5$ but eventually it will drop back into the potential-mould to its left or to its right. This explains, why in fig. 3 at $T = 4.00$ the curve looks like a twisted 8: The two closed arcs left and right of $x = 0.5$ is the particle traveling in the left resp. right potential mould. For higher temperatures (e.g. $T = 10.0$), the particle has that much energy, that the potential hill cannot stop it but only slows it down a little.

1.4 Andersen Thermostat

We varied the parameter ν controlling the probability with which a (the) particle will receive an energy-kick. In the plots of fig. 6 you can observe, that for small ν there are distinct arcs – the particle propagates on a phase-space-shell. The larger ν is, the shorter the arcs are. For $\nu \sim 1$ the arcs vanish completely: The probability to receive a kick is now that large, that

¹You can see this by looking at how close the points are to each other around $x = 0.5$ – the particle rests quite long in this area and thus produces many measurements there.

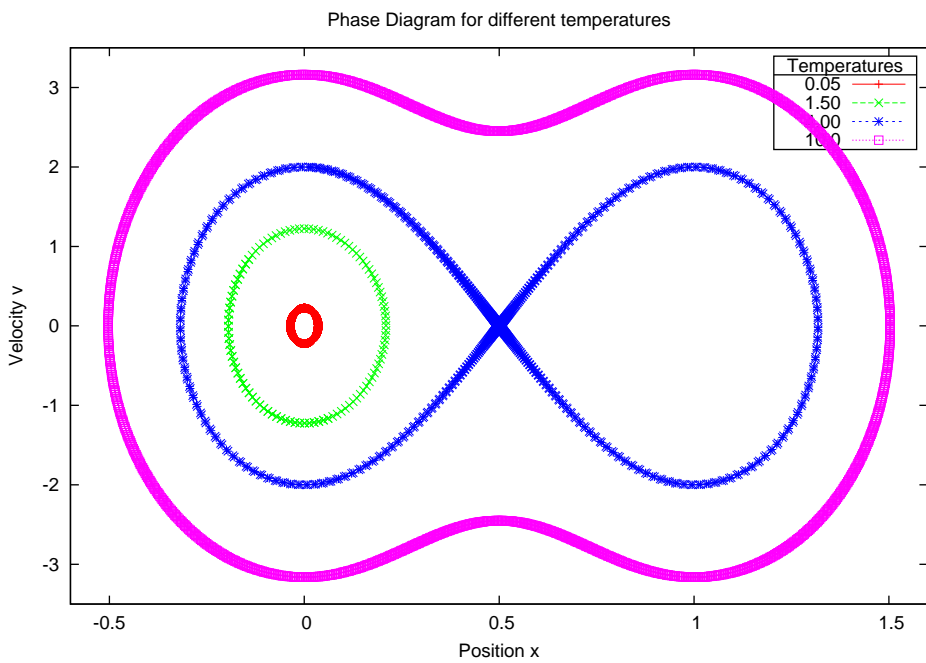


Figure 3: Phase diagrams for different Temperatures

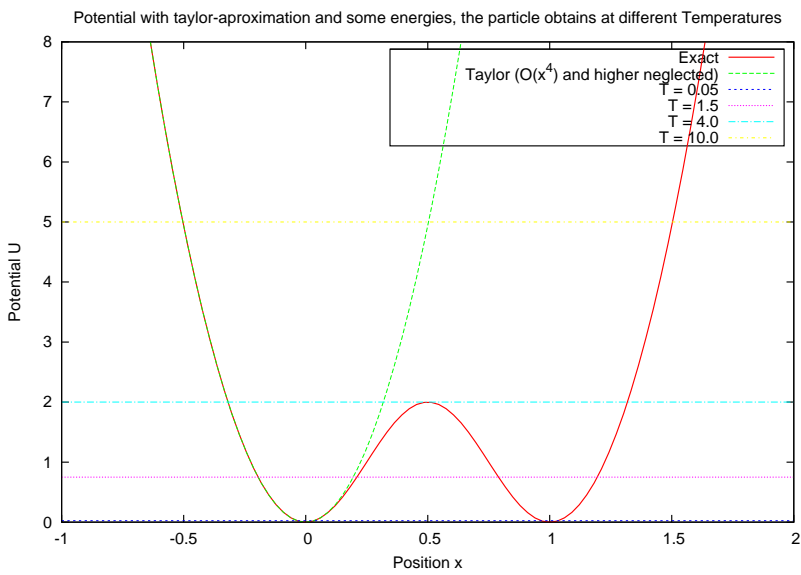


Figure 4: Potential (1) with Taylor-approximation (2) and the energies of particles at some Temperatures – compare fig. 3. $T = 2E_k$ was used here...

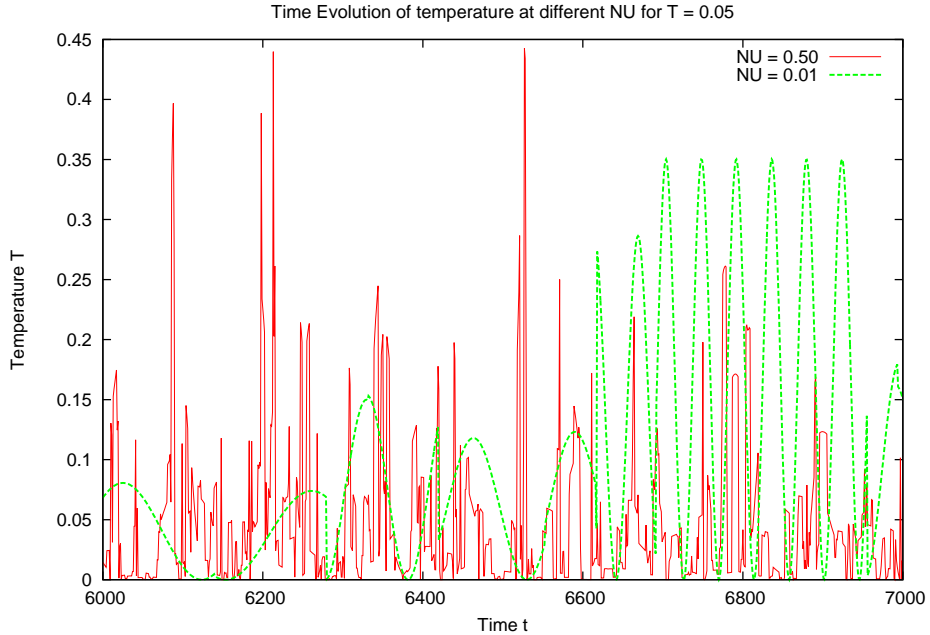


Figure 5: Instantaneous kinetic temperature with the Andersen thermostat at $T = 0.05$ for different ν .

the particle cannot travel undisturbedly for several timesteps in a row and thus cannot follow an arch. For $\nu \geq 1$ the propagation in the phase-space is nearly perfectly random (or at least not distinguishable with bare eyes).

In fig. 5 you can see the temperature in the System with Andersen thermostat. The temperature fluctuates very much. This is due to the fact, that every now and then the particle receives or loses some kinetic energy and thus since

$$T \propto E_k$$

also the kinetic temperature increases resp. decreases. In the $T = T(t)$ -diagram you can see that in small time-segments the temperature follows some smooth curve – here the particle propagates undisturbed in the potential (1), until the Andersen thermostat speeds it up or slows it down. In the plot with $\nu = 0.01$, these segments are large and in the one with $\nu = 0.5$ they are so small, that they are almost invisible. So we can see again clearly that a larger ν produces a more random movement since the particle is kicked quite often.

I used a script looping over different values of NSTEP for several times (at

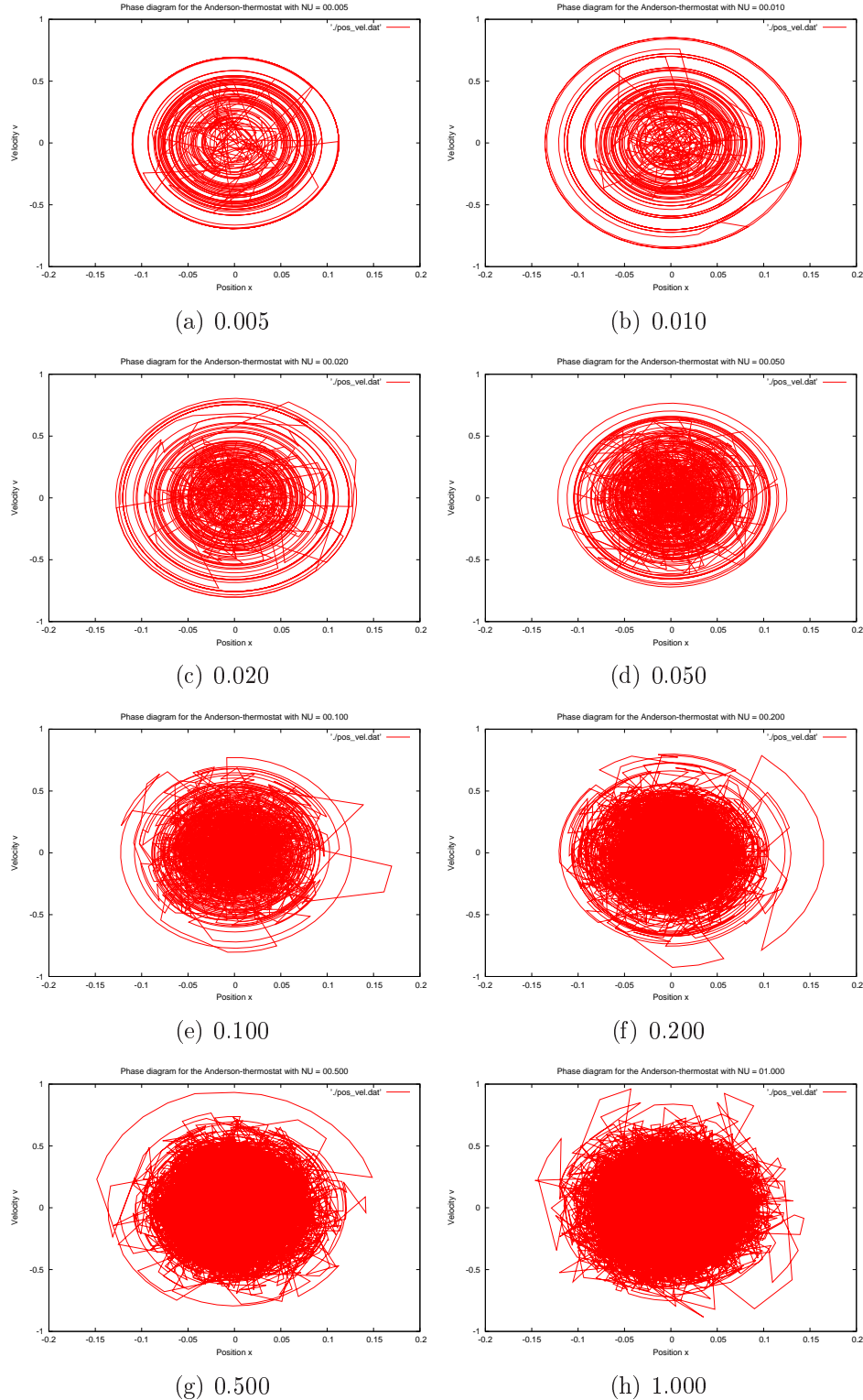


Figure 6: Phase diagram of the Andersen thermostat for different coupling parameters ν , T was set to $T = 0.05$ and timestep was 0.01. For $\nu = 0$ cf. fig 2.

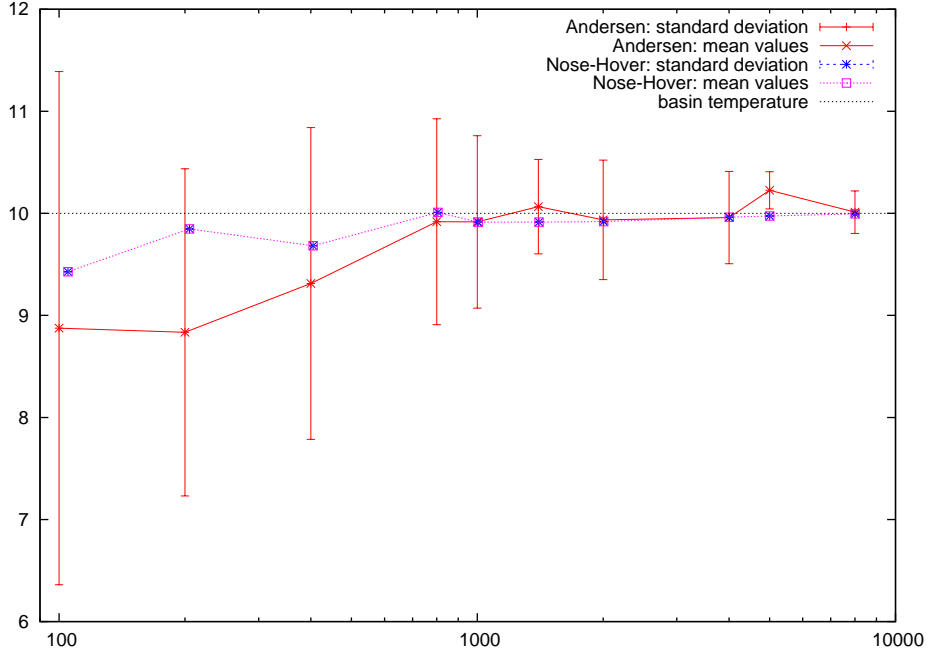


Figure 7: Average Temperature for different numbers of NSTEP

least 20 times, more often for smaller NSTEP), storing each time the Average Temperature and NSTEP. We used a timestep of 0.01, a basin temperature of 10 and $\nu = 0.05$ for Andersen. The output was then treated using octave: The mean average Temperature and it's standard deviation was computed. This was done once using the Andersen thermostat and once using the Nose-Hover thermostat. The results are presented in fig. 7.

You can see, that both the Andersen and the Nose-Hover thermostat need a number of Steps to get to the averaged temperature we desire. Andersen takes longer to do so, but not much longer. Far more interesting is the statistical behaviour of Andersen: The standard deviation for small NSTEP ($\sim 10^2$) is very large, and it decays for larger NSTEP only moderately fast – it shrank to about 1/4 for NSTEP = 8000, which is still quite large.

The Nose-Hover thermostat on the other hand does not show any statistical behaviour. The average temperature converges a little bit faster to the desired one. But on the other hand the Nose-Hover algorithm took much longer time than Andersen.

We know from the analytical solution, that the particle will have sufficient energy to cross the barrier at $T = 4$, yet using Anderson the particle will

from time to time receive an energy-kick which lifts it over the barrier. It may then propagate in the second potential-well or get back again.

To check, at which temperature the particle will most likely begin to cross, we ran a simulation using the Andersen thermostat with $\text{NU} = 0.05$ for $\text{NSTEP} = 1000$ at $\text{TSTEP} = 0.01$ for different temperatures in between 0 and 1; each one at least 200 times (in the area 0.2 to 0.8 300 times). In each simulation, the value of the density at $x = 0.7$ was taken. The values for one specific temperatures were summed up and in the end divided by the numbers of loops at one temperature. Thus we received some probability, indicating how much of his time the particle spends in a certain space which is across the potential wall.

The results are presented in fig. 8. As you can see, the data is scattered rather much for larger temperature, but does follow some distinct “global” behaviour. We used an arctan-Function to illustrate this. Using this fit, we can state that for temperatures larger than $T_1 == 0.330392 \pm 0.004452$ the particle will more likely cross the boundary than it will not. Examining the data files yields, that the particle *starts* (there the probability to be in the segment across the “border” is nonzero the first time) at $T_2 \sim 0.2$ to cross the border.

This is a rather astonishing since the temperature is eight times smaller than the “analytical” solution would suggest. To check, how much this value depends on NU of our Andersen thermostat the simulation was conducted a second time using $\text{NU} = 0.15$ and a third using $\text{NU} = 0.25$. They are plotted in fig. 9 and as you can see the observations from fig 8 almost hold: The particle starts to cross the wall at about the same temperature but you can see, that the temperature, when the particle will be more likely over the optential than not to be shifted towrads lower temperatures for larger NU. This is totally understandable since for larger NU it’s more probable for the particle to receive his “crucial” kick. For the same reason the curves for larger NU are a little steeper.

2 Langevin Thermostat in a Lennard-Jones Liquid

2.1 Velocity Verlet Algorithm

Although our system follows the Langevin-equation

$$m\mathbf{a} = \mathbf{F} = m\gamma\mathbf{v} + \mathbf{W}(t) \quad (3)$$

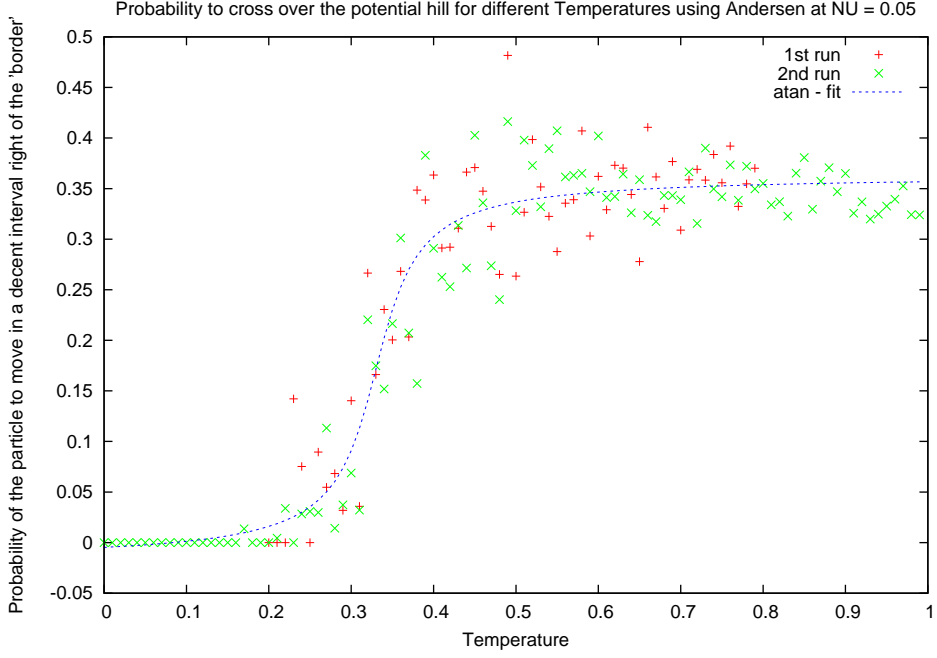


Figure 8: Probability of the particle to cross the potential wall.

where $\mathbf{W}(t)$ is a stochastic force with

$$\langle W_i(t) W_j(t') \rangle = \delta_{ij} \delta(t - t') \cdot 5k_B m T \gamma$$

and $m\gamma v$ a friction, we use the Velocity Verlet algorithm which requires a Hamiltonian (which especially conserves energy) system...

The Velocity Verlet integrator is ($v' = v(t + dt)$ indices are not explicitly written to enhance legibility):

$$v' = v + \frac{a + a'}{2} dt . \quad (4)$$

If we substitute a and a' for the corresponding terms derived from eq. (3) ($a = G/m - \gamma v$ where $G = F + W$) we get

$$v' = v + \frac{G/m - \gamma v + G'/m - \gamma v'}{2} dt .$$

By adding $\gamma v' dt/2$ and pulling $-\gamma v dt/2$ out of the fraction we obtain by simple factorisation

$$v'(1 + \gamma dt/2) = v(1 - \gamma dt/2) + \frac{G + G'}{2m} dt$$

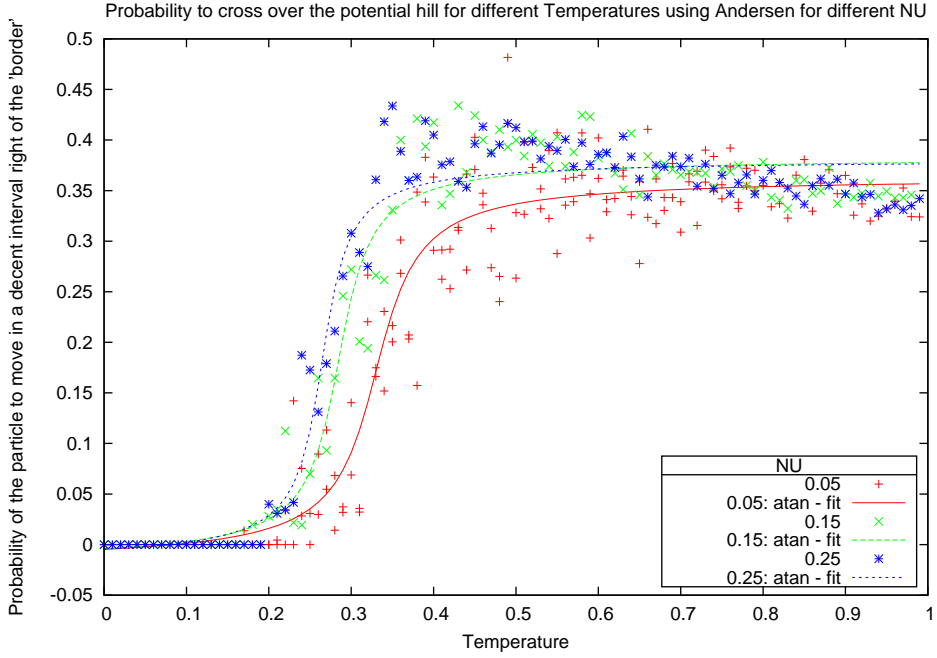


Figure 9: Like 8 but for three different NU

and thus the integrator we will implement is

$$v' = \frac{v(1 - \gamma dt/2) + \frac{dt}{2m}(G + G')}{1 + \gamma dt/2}. \quad (5)$$

2.2 Energies

A run with 10000 timesteps was done. The time-evolution of energies was plotted in fig. 10. We could think, that the total energy in the simulation without friction ($\gamma = 0$) was conserved – but if you look at 10(b), you can see, that the conserved-looking total energy does fluctuate, too although on a very small scale ($\Delta E/E \sim 0.05/600 \approx 8 \cdot 10^{-5}$ while $\Delta E/E \sim 60/340 \approx 0.17$ for the total energy with friction ($\gamma = 1.0$)): This seems to be computer precision, so the energy is conserved for a system without friction.²

²Actually I would have expected some fluctuation due to the random nature of the force \mathbf{W} : If you use $\gamma = 0$ in (5) you get the “classical” Velocity Verlet algorithm but this should conserve energy only in systems where $\mathbf{F} = -\nabla U$ with $U = U(\mathbf{r})$. Further investigation showed, that $W = \sqrt{12} \sqrt{2\gamma T_b/p}$, so $\gamma = 0 \Rightarrow W = 0$, and everything’s fine again

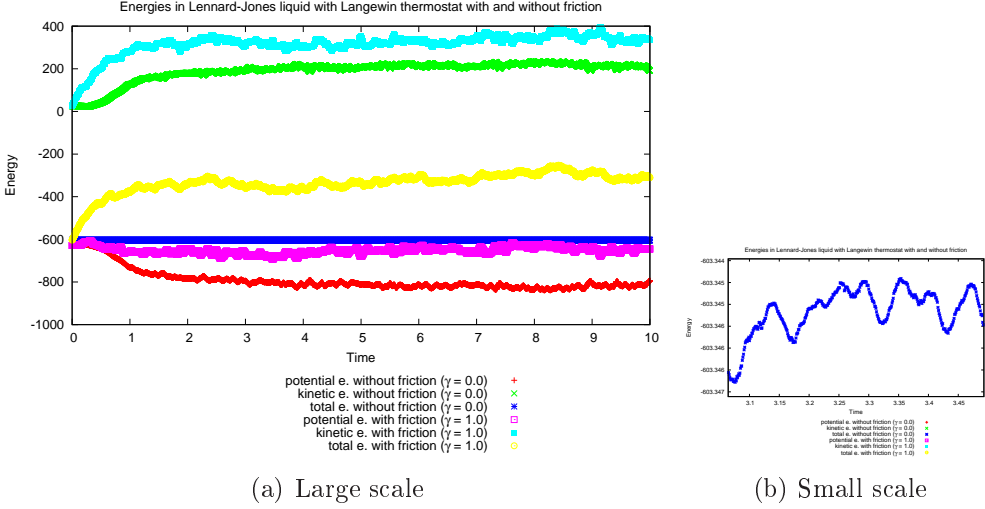


Figure 10: Energies in a Lennard-Jones simulation with Langevin thermostat.

In fig. 11 you can clearly see, that the system will tune to the desired temperature depending on parameter γ : The larger γ , the faster the temperature converges towards the bath temperature. To verify, that even for small γ the temperature does converge, cf. fig. 11(b): Here $\gamma = 0.1$ and $\gamma = 1.0$ are plotted. Obviously with both frictions the temperature converges to the (desired) bath temperature and in both cases the fluctuation of the temperature (due to the random forces) has about the same amplitude. The process of convergence is slower with smaller γ since the random forces with $W = \sqrt{12} \sqrt{2\gamma T_b/p}$ are smaller and thus cannot affect the particles velocity as much as a larger force could.

2.3 VACF and MSD

The simulation was performed several times using the parameters

```
. /lan_thermo -dt 0.0001 -ns 30000 -fs 10 -Tb 1 -uf -rho
XXX
```

where XXX denotes the changed parameter of the density. The produced .xyz-files were examined using the program `diffusion.c`. The resulting VACFs are displayed in fig. 12 and the MSD in fig. 13.

We're basically considering a diffusion process. EINSTEIN showed, that

$$2D = \frac{\partial \langle r^2(t) \rangle}{\partial t} \quad (\Leftrightarrow 2Dt = \langle r^2(t) \rangle) \quad (6)$$

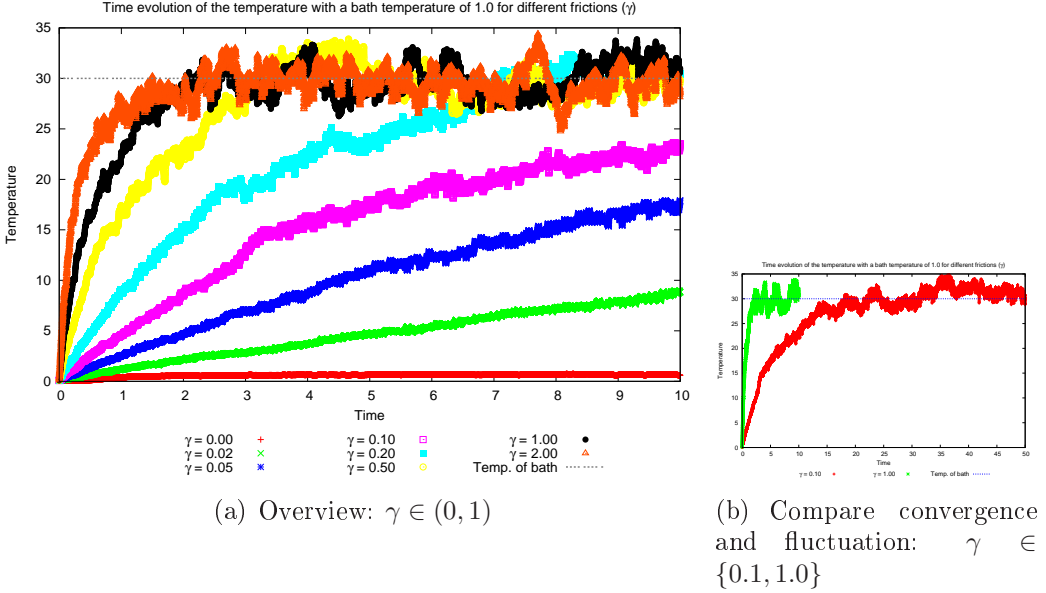


Figure 11: Time evolution of temperatures with the bath-temperature set to 30 for different γ

holds, where D is the diffusion constant. So in equilibrium we expect, that the MSD $\partial\langle r^2(t)\rangle$ is linear; fig. 13 confirms that.

In the MSD you can relatively clearly see two “regimes”; two linear correlations with different slope. For large densities there are even three ones.

The first of these regimes is called *ballistic*, since the particles are at the beginning of the simulation moving rather randomly, bouncing off each other etc. It takes some time, until they will find into an equilibrium – then (6) holds and we get the desired proportionality. Bear in mind that the diagram is a log-log-one, so the first straight line in 13 means, that $\langle r^2(t)\rangle \propto t^\alpha$ with $\alpha \neq 1$.

We can rewrite eq. (6), using $r = \int v dt$: The averaging in (6) then becomes

$$\left\langle \left(\int v dt \right)^2 \right\rangle = \int_0^T dt \int_0^T dt' \langle v(t) \cdot v(t') \rangle = 2 \int_0^T dt \int_0^t dt' \langle v(t) \cdot v(t') \rangle \quad (7)$$

which is the autocorrelation function (since we assumed to be in equilibrium, only the difference $\tau := t - t'$ may be important, so $\langle v(t) \cdot v(t') \rangle$ becomes $\langle v(\tau) \cdot v(0) \rangle$, which (at least for me) is the *true* autocorrelation function). (6)

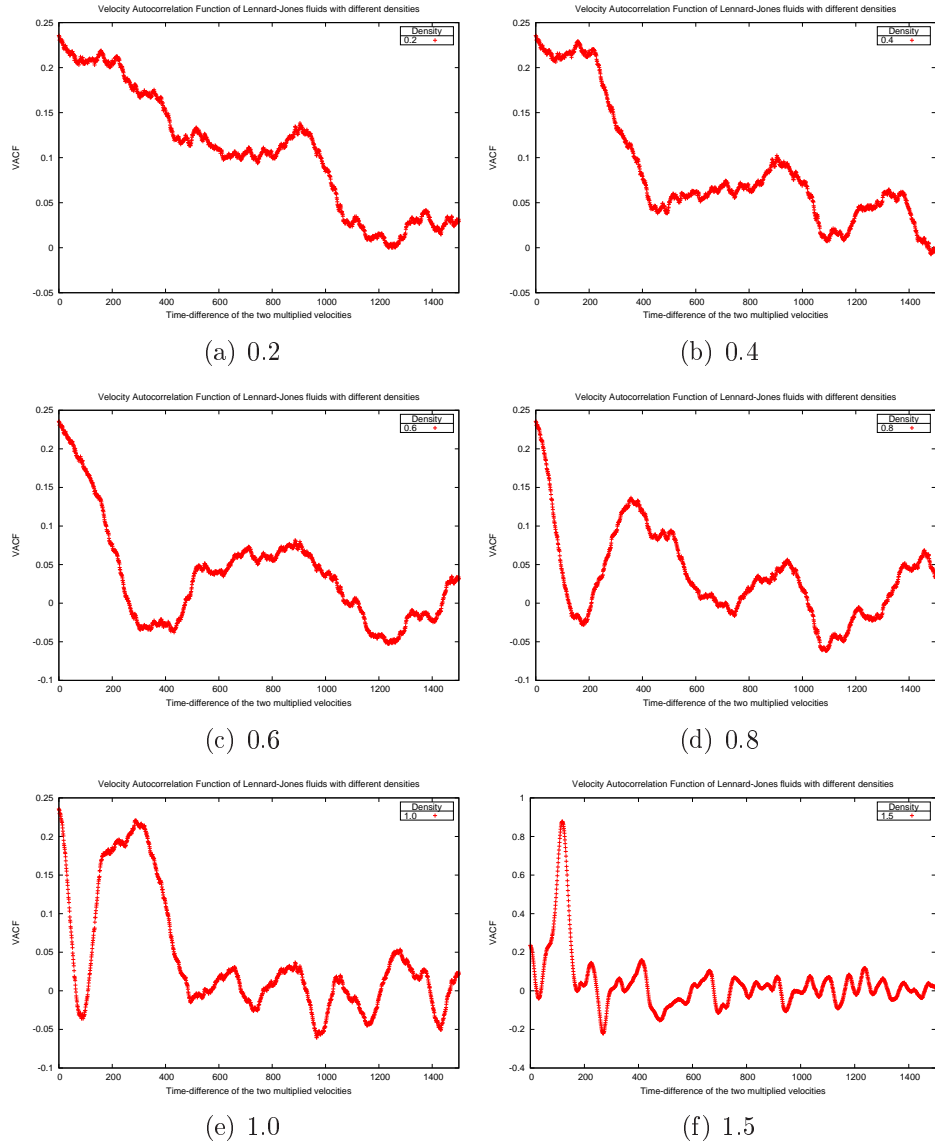


Figure 12: Velocity Autocorrelation Function for different densities – the density (in reduced units) is written in the captions

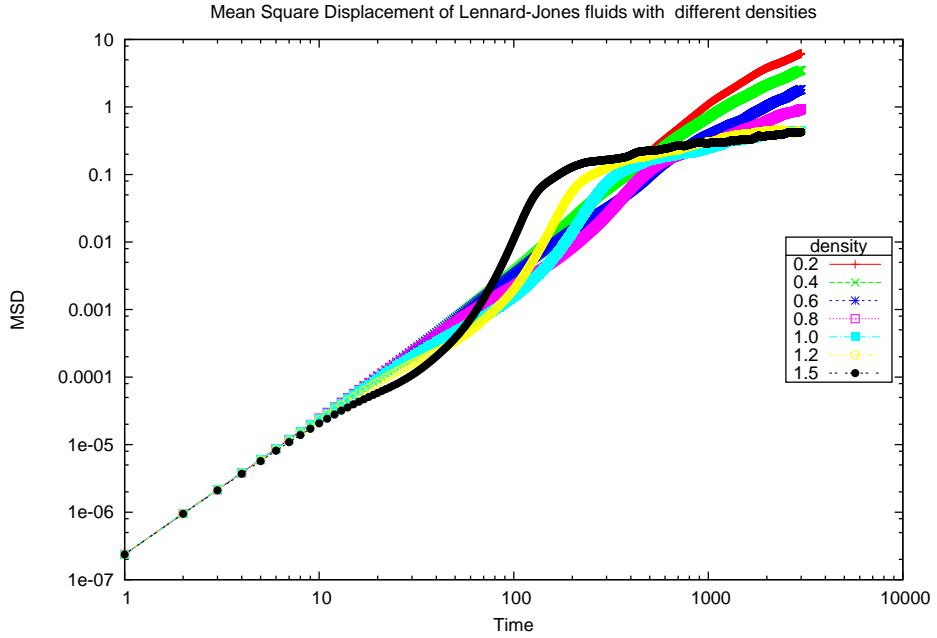


Figure 13: Mean Square Displacement for different densities

then becomes

$$D = \int_0^\infty d\tau \langle v(\tau) \cdot v(0) \rangle . \quad (8)$$

This tells us, that we should expect³ the VACF to oscillate around 0 – which is backed up by fig. 12.

The more the VACF oscillates, the stronger are the forces in the system: Without forces we would have no change in velocity and thus the VACF a horizontal line; with small forces the product $v(\tau) \cdot v(0)$ slowly decays as v gradually changes (this is partially what we see for $\rho = 0.2$). In our simulation these stronger forces occur if the particles are near to each other, thus in more dense systems. Here the particles oscillate around the mechanical-equilibrium-points (equilibrium between repulsive and attractive forces). The more dense the more stable these positions are and the more oscillatory is their motion. That's why the oscillation is the strongest for $\rho = 1.5$ and the lowest for $\rho = 0.2$.

³Since D is a fixed value but the integral is computed over $[0; \infty]$, the area above and under the VACF=0-Axis must be equal. One solution to this constrain is an oscillation.